NEW BEARING STEEL FOR HIGH-SPEED APPLICATIONS

CHRISTIAN BRECHER, STEPHAN NEUS, MARCUS GAERTNER

Laboratory for Machine Tools and Production Engineering (WZL) of RWTH Aachen University, Germany

LEONARDO CATANA, FELICIANO GRECO, GUILLERMO MORALES-ESPEJEL, DEFENG LANG

SKF, Gothenburg, Sweden

DOI : 10.17973/MMSJ.2021_12_2021129

m.gaertner@wzl.rwth-aachen.de

The requirements for speed suitability and fatigue strength of motor spindle bearings are constantly increasing. These challenges can be met by further developing the spindle bearings, e.g. by using higher-performance bearing steels. In the following, the experimental investigation results of a spindle bearing made of a new raceway steel tested on a high-speed rolling bearing test rig are presented. Spindle bearings of the type 7008 (hybrid execution) were tested in an endurance run at a rotational speed of 46 krpm and 3 kN axial load. The operating behaviour was validated based on the bearing outer ring temperature and the vibration behaviour. Microscope analysis of the raceways after the test shows that the new steel has good resistance to micropitting and surface fatigue. The calculated contact pressures, wear parameter and lifetime for the bearings in the tests show that the performance limits of spindle bearings are significantly higher than initially assumed.

KEYWORDS

Spindle bearings, test rig, bearing steels, contact pressures, wear parameter, lifetime prediction, motor spindles

1 INTRODUCTION

Increasing the speed suitability of spindle bearings for high-speed cutting (HSC) is an important research topic. In aerospace engineering e.g., the trend is to mill larger components with high cutting volume [Brecher 2017]. The high cutting speeds and high feed rates that are applied require a high speed suitability, load capacity and stiffness of the bearings. The high-precision bearings used in the spindle are characterised by low run out errors and typically achieve speed parameters nxd_m of up to 2.7 million mm/min [SKF 2014]. In order to meet the increasing requirements, more efficient bearings must be developed and tested. Various approaches have been investigated, e.g. by coating the rolling elements and rings, optimizing the contact geometries or lubrication of the bearings [Spachtholz 2008 ; Rossaint 2013 ; Gerlach 2014]. In other approaches, the use of higher performance bearing materials has proven to be successful. For aerospace applications, hybrid spindle bearings with Cronidur 30 steels have gained acceptance due to their corrosion resistance, higher load capacity, operating temperatures and service life [Bayer 1998]. With bearing rings made of Cronidur, for example, the fatigue strength limit has been increased to 2,800 MPa. The fatigue strength limit for standard steel spindle bearings made of 100Cr6 in comparison to hybrid cronidur bearings is only 1,500 MPa [ISO 281]. A further increase in operating life can be achieved with Vacrodur bearing rings. With bearing rings made of Cronidur, despite of having slightly lower hardness, they have higher fatigue limit compared with standard steel [Ragen 2002].

Adhesive wear is initially dominant and can lead to an early failure. For high rotational speeds a stable lubricant film is important to minimise surface fatigue. In addition, the speed suitability can be increased by using a new bearing steel (SKF PM1), which was introduced in [Sherif 2021] and [Morales-Espejel 2021]. The experimental test results of this new bearing steel are presented in the following.

2 EXPERIMENTAL METHODS AND RESULTS

2.1 Test bearings

Eight hybrid spindle bearings of the type 7008 with a contact angle of 18° were tested. The limiting speed of the bearings for an oil-air lubrication is 56 krpm. The balls consist of silicon nitride, the bearing rings are made of powder metallurgy bearing steel (PM1). The steel composition, thermal conductivity λ and Rockwell hardness RH of the new steel (PM1) and the reference steel (100Cr6) are given in Table 1.

	Steel composition in wt%					λ [W/mK]	RH [HRC]
	C	Cr	Mo	V	Si		
PM1	1.4	4.7	3.5	3.7	0.4	33.5	61.9
100Cr6	0.9	1.5	0.03	-	0.3	32.2	61.4

Table 1 : Properties of the steels [Morales-Espejel 2021, Sherif 2021]

The tolerance class of the bearings is 4 in accordance with ISO 492:2014 [ISO 492:2014]. The geometrical data for this bearing type are given in Figure 1.

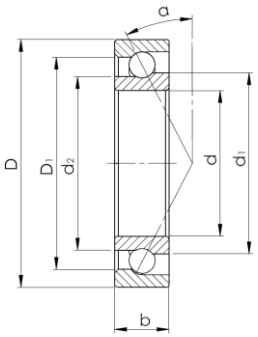

Inner diameter inner ring d	40 mm
Outer diameter outer ring D	68 mm
Width b	15 mm
Outer diameter inner ring (shoulder) d_1	49.7 mm
Outer diameter inner ring d_2	47.6 mm
Inner diameter outer ring (shoulder) D_1	58.25 mm
Contact angle α	18°

Figure 1. Geometric data of the test bearing according to [SKF 2014]

2.2 High-speed bearing test rig and test program

The general concept of the test rig is characterised by its high modularity, so that different bearing types and sizes can be investigated with a few modifications on the test rig, which is described in [Falker 2020]. The test rig for the investigation of the prototype bearings is shown in Figure 2.

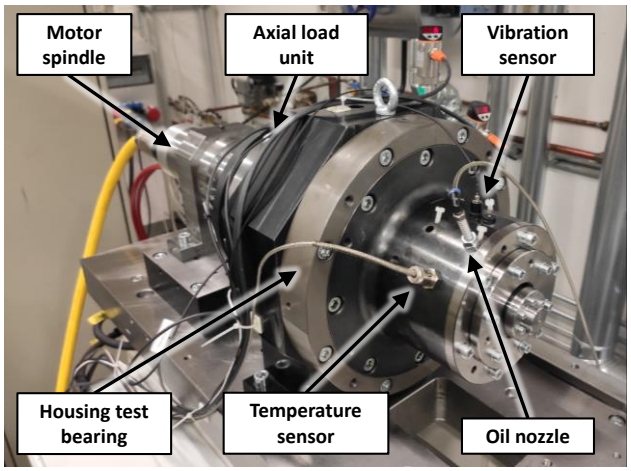

Figure 2. High speed bearing test rig

The shaft is driven by a motor spindle, which can reach a maximum speed of 60 krpm. During the bearing tests the temperature on the outer ring is measured by a resistance thermometer. Furthermore, the vibrations of the test rig are measured with a piezoelectric acceleration sensor mounted on the housing.

The test rig in its cross-sectional view with the force flux through the test bearings is shown in Figure 3. In this configuration, the parallel testing of two test bearings is possible, whereby the back bearing is mounted in an axially moveable sliding bush. The axial preload force is applied by hydraulic cylinders and is controlled on a constant level by the feedback signal from the force sensors. To ensure sufficient lubrication at the relatively high speeds, the two bearings were lubricated with 240 µl/h. A finely filtered synthetic spindle bearing oil of the viscosity ISO VG 68 is used as lubricant. To avoid an oil accumulation in the bearing in the endurance run, which can lead to increased fluid friction and higher temperatures, both bearings are provided with an oil suction system.

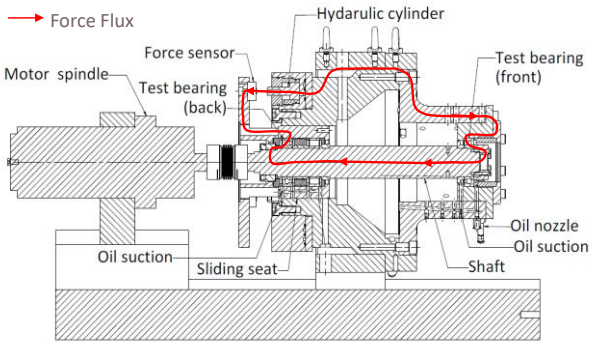

Figure 3. High-speed bearing test rig – cross section

The test conditions for the investigated bearings are given in Table 2. The shaft and the coupling were balanced in order to minimize vibrations due to imbalances for this speed range.

Rotational Speed n [krpm]:	46
Axial load F_{ax} [kN]:	3
Test duration t_d [h]:	432
Lubrication quantity q [µl/h]:	240

Table 2. Test conditions of the bearings

2.3 *Running-in behavior of the bearings*

The run-in procedure has a great influence on the success of the experiment. To ensure sufficient lubrication during the start, the bearings are pre-lubricated for 12 h with the lubrication quantity q of 240 µl/h before each test. To keep the starting torque low, the load was applied stepwise. In order to ensure sufficient preload, an axial load F_{ax} of 1 kN is first applied at standstill, after approaching 2 krpm the axial load is increased and then the speed step of 5 krpm is approached. Afterwards, the load is increased to 3 kN and the speed to 10 krpm, before the target speed of 46 krpm is reached in the last step.

The high-frequency sampled acceleration signals can be evaluated in the form of an RMS value and help to assess the dynamic behaviour of the test rig during an endurance run [Brecher 2017]. The exemplary run-in procedure of the test with the acceleration behaviour a_{RMS}, the axial load F_{ax} and the nominal rotational speed n_{nom} of the bearing are shown in Figure 4. To minimize the influence of hitting possible natural frequencies and to avoid a possible pre-damage of the bearing, the target speed was reached within a few seconds. With this procedure, resonance effects can be minimized for the critical rotational speeds n_{crit} of 18 krpm, 22 krpm and 38 krpm, where the acceleration peaks are passed for a short time (see Figure 4).

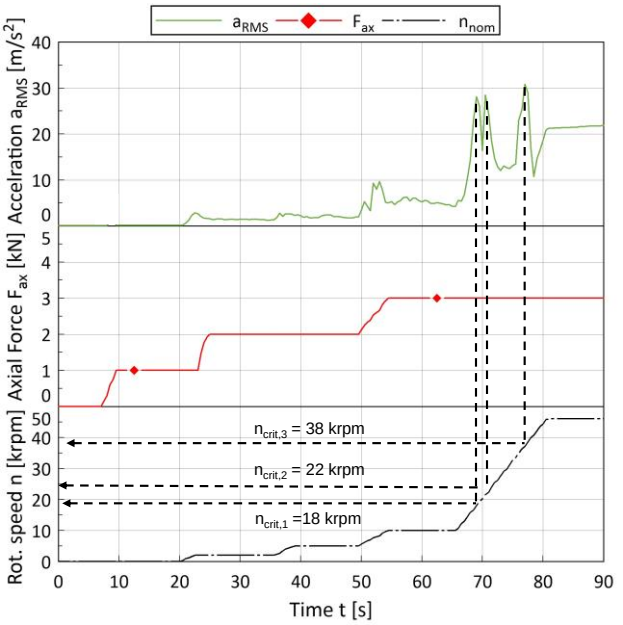

Figure 4. Run-in procedure

2.4 *Temperature behavior during the endurance run*

The outer ring temperature of three test bearing pairs during the test runs are shown in Figure 5. The first abbreviation *f/b* stands for the position of the bearing, i.e. front/back, and the last number indicates the test number. In general, the test bearings, both front and back, show a constant temperature level during the endurance runs. The temperature level of the front test bearings fluctuates about 60 °C to 62 °C, the temperature level of the back bearing tends to be higher at about 70 °C to 72 °C. The increased temperature at the back bearing compared to the front bearing can be explained due to the significantly poorer heat dissipation at the back bearing. Compared to the front bearing, the back bearing is surrounded by massive housing mass, which heats up during the test, resulting in a lower temperature gradient and poorer heat dissipation. The greater fluctuations in the temperature level are due to the different flow conditions during injection. At the back bearing, due to the smaller bore channels, higher dynamic pressures prevail at the injection nozzle, which lead to greater fluctuations in the oil shear supplied, so that the effectively injected oil quantity fluctuates more compared to the front bearing.

Furthermore, a shortened test run with standard hybrid bearings (Reference) of 48 h was carried out as a reference for the prototype bearings, which is also shown in Figure 5.

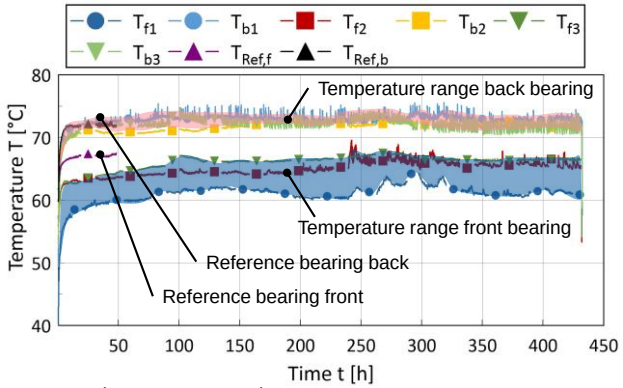

Index: f/b: Position (front/back), i: Test number

Figure 5. Outer ring temperature of the test bearings

The two standard bearings (Reference) reach a similar temperature level to the prototype bearings in the shortened endurance run, whereby the front standard bearing is slightly above the level of the prototype bearings with a steady-state temperature of about 67 °C. The different temperature levels can be attributed to the slightly different geometries of the bearings.

2.5 Vibration behavior during the endurance run

The measured acceleration signals can be used to assess the condition of the machine and its bearings. In some approaches, the acceleration values are used to validate the lubrication condition in the bearing [Brecher 2020]. Damage occurring in the bearing can thus be detected at an early stage. However, relatively high sampling rates of 10 kHz till 25 kHz are required to detect the natural frequencies of the bearings and their changes. A reduced indication of the vibration level is provided by the RMS value. This value has proven to be useful for characterising the condition of the spindle bearing and is calculated with equation (1) as follows [Cantelbajac 2014]:

$$a_{RMS} = \sqrt{\frac{1}{N}\sum_{n=0}^{N-1}(x(n)-\bar{x})^2} \quad (1)$$

where $\bar{x}$ stands for the time average of the time series $x(n)$. The acceleration behaviour and the vibration velocities of the bearing tests is shown in Figure 6. In all three test runs, a constant vibration level below 50 m/s² is reached after 100 h at the latest. This is caused on the one hand by the smoothing of the roughness peaks in the raceways and on the other hand by the almost isothermal conditions in the bearing due to the reaching of a temperature steady state. To classify the vibration velocities, the recommendation according to the ISO 10816-3 standard is not to exceed a vibration velocity of 4.5 mm/s in continuous operation with reference to the test rig [ISO 10816-3]. In the case of the tests with the prototype bearing, the vibration velocities are largely at the recommended level of the standard. The velocities with the shortened run with the reference bearings are significant above the specified limit of the DIN standard.

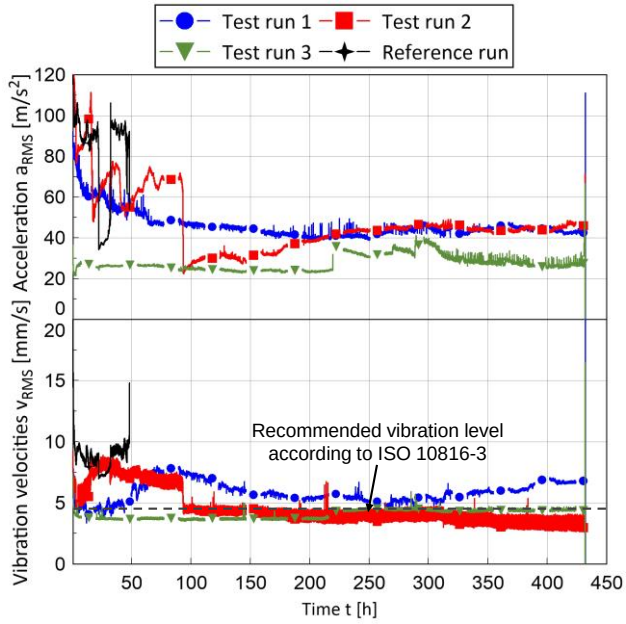

Figure 6. Acceleration and vibration velocities of the test bearings

2.6 Microscopic analysis of the bearings

Figure 7 shows exemplary views of the inner ring raceway of the front and back bearing of bearing f3 and b3. The raceway is slightly brownish discoloured in the area of contact with the ball and indicates oxidation reactions with the lubricant due to higher temperatures in the contact. The raceway of the back bearing is much more widely discoloured, which is also consistent with the higher temperatures measured for the back bearing. Wear cavities in the raceway could not be detected by means of tactile measurements of the surface contour across the raceway.

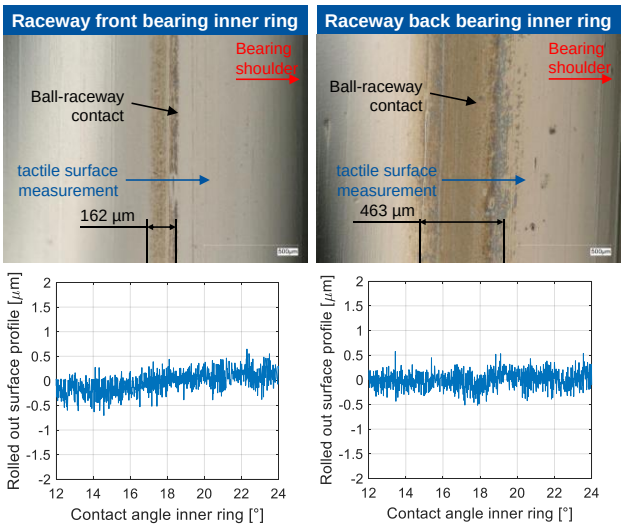

Figure 7. Microscopic views of the inner ring raceway

In [Sherif 2021] the wear patterns of a micropitting damages are classified by investigations on a micropitting test rig. A comparison of the back bearing from test 3 with the micropitting resistance scale described in [Sherif 2021] shows that the new steel of the tested bearings has good micropitting resistance. In the following, the operating behaviour with the conditions in rolling contact is analyzed in order to classify the measured wear pattern and the experimental results.

3 ANALYSIS OF THE OPERATING CONDITIONS

3.1 Simulation model

To evaluate the operating conditions of the bearings in the test rig, simulations with the MATLAB based program MTPlus were carried out. This program enables the coupled calculation of the operating behaviour of the shaft and the bearings in a holistic approach [Brecher 2019]. The general calculation process in MTPlus is shown in Figure 8 [Falker 2020].

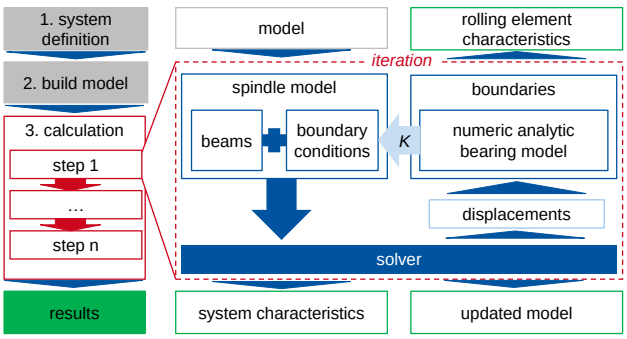

Figure 8. Calculation process in MTPlus [Falker 2020]

In the first step (1. system definition), the geometry elements and boundary conditions are defined. The geometry elements are e.g. the shaft and the housing, which are considered as FEM

beams. The characteristics of the bearings, which are modelled as a spring-damper elements, are taken into account in the boundary conditions. In the second step (2. build model), the shaft bearing model is created, whereby the properties of the geometry elements and boundary conditions are approximated. In the calculation process (3. calculation), the forces applied to the spindle and bearings are iteratively determined using the following general equation (2).

$$\{F\} = [K]\cdot\{q\} + [C]\cdot\{\dot{q}\} + [M]\cdot\{\ddot{q}\} \quad (2)$$

The force vector F results from the matrices of the system stiffness K, the system damping C, the system mass M as well as from the vectors of the node displacement q, velocity $\dot{q}$ and acceleration $\ddot{q}$. The non-linear bearing properties are included in the equation in the form of the stiffness matrices K. In each iteration step the stiffness matrices K of the rolling elements are updated. The results of the calculations are the rolling element characteristics, such as the contact pressure, contact angle and normal forces, as well as the system characteristics and the updated model. This approach allows an accurate characterisation of the operating behaviour of the bearings in combination with the thermal characteristics of the spindle and the housing during the tests carried out.

The simplified set-up of the shaft bearing system in this program is shown in Figure 9.

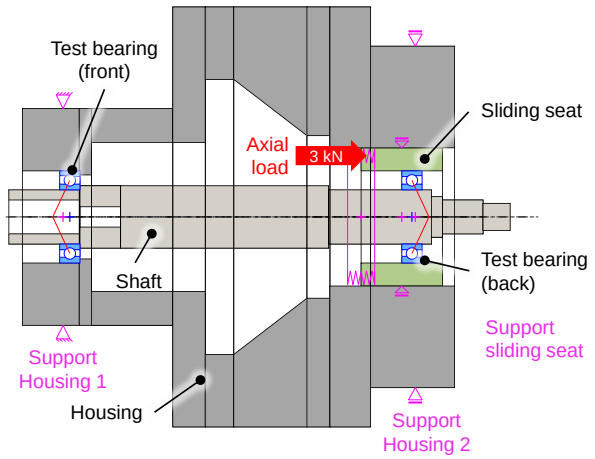

Figure 9. Simulation model of the test rig in MTPlus

In the model, the measured bearing geometries were taken into account as well as the measured temperatures on the outer ring. Hybrid bearings with bearing rings made of 100Cr6 steel were simulated. For the front bearing, an outer ring temperature of $T_{OR,f}$ = 61 °C was assumed, for the back bearing a temperature of $T_{OR,b}$ =72 °C and for the shaft a temperature of T_{Shaft} = 80 °C was estimated.

3.2 Contact pressures and ball kinematics

In order to classify the operating behaviour, the maximum contact pressures p_{max} in the rolling contact were calculated, which are shown in Figure 10. Especially for the critical inner ring contact, contact pressures of 2,876 MPa are significantly above the fatigue strength limit of 1,500 MPa customary for spindle bearings [ISO 281]. Based on the test results for the bearings with the new PM1 steel, a higher fatigue strength limit can be assumed. The spin-to-roll ω_r/ω ratio is also an important design parameter for spindle bearings. This ratio describes the ratio of the spinning speed and the rolling speed at the respective ball-bearing ring contact [Brecher 2017]. The calculation results of the spin to roll ratio are shown in Figure 10. In the case of the test bearings spin to roll ratio with a maximum of 9 % is not critical.

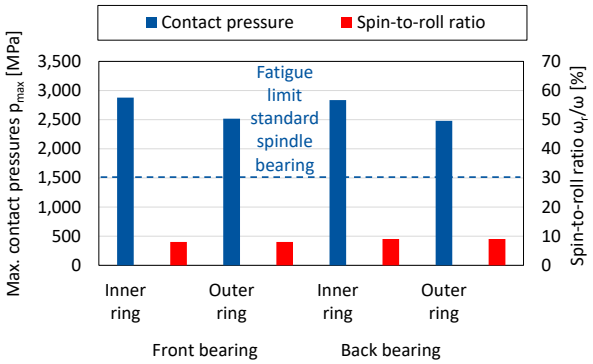

Figure 10. Contact pressures and spin to roll ratio

3.3 Wear parameter

Past works have shown that the wear parameter pv_{rel} is an important design parameter for rolling bearings [Hentschke 2012, Heinz-Schwarzmeier 2003]. This parameter is the product of the contact pressure p and relative speed v_{rel} and characterises the energetic energy transfer in the rolling contact. The local distribution of the wear parameter in the rolling contact is shown in Figure 11.

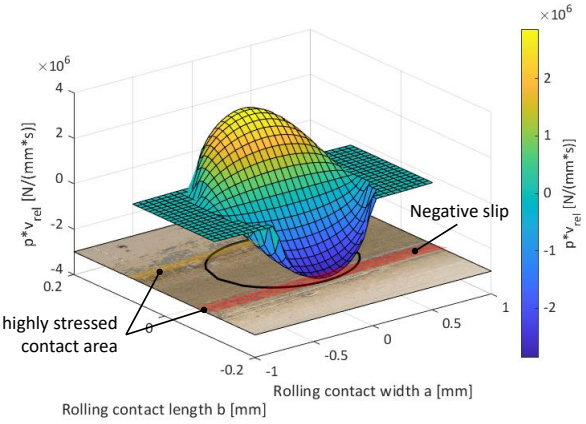

Figure 11. Wear parameter in the rolling contact of the inner ring

In the areas of the absolute maxima of the wear parameter, the rolling contact is highly stressed and wear is to be expected in these areas. Particularly in the area of negative slip, where the inner ring and roller slide in opposite directions, increased wear can be expected at higher loads [Hentschke 2012]. With an increasing speed parameter, the frictional energy input in the rolling contact rises, which leads to a reduced tribological load limit. In [Morales-Espejel 2019], a correlation between the maximum contact pressure and the increasing speed parameter for hybrid spindle bearings is presented, which illustrates that the wear parameter in the bearing tests is comparatively high.

3.4 Lifetime calculation

The calculated lifetime L is also a suitable design parameter to validate the test condition. The theoretical value, which is based on statistical assumptions, describes the time in hours or load cycles when a bearing failure due to fatigue can occur with a certain probability. The lifetime calculation is standardized in ISO 281 [ISO 281] and ISO/TS 16281 [ISO 16281]. With ISO 281, the basic rating lifetime L_{10h} of the bearings can be quickly estimated with 90 % reliability for normal manufacturing qualities and operating conditions with equation (3).

$$L_{10h} = \left(\frac{C_r}{P_r} \right)^p \quad (3)$$

The basic dynamic load rating C_r is a bearing-specific value that is specified by the manufacturer. The exponent p depends on the bearing type (balls: 3, rollers: 10/3). The dynamic equivalent bearing loads P_r results from the axial force F_{ax} and radial force F_{rad} applied on the bearing and is determined by bearing-specific weighting factors X and Y with equation (4).

$$P_r = X \cdot F_r + Y \cdot F_{ax} \quad (4)$$

When the reliability and the influence of the lubricant have also to considered, the modified rating lifetime L_{nmh} can be calculated with equation (5).

$$L_{nmh} = a_1 \cdot a_{iso} \cdot L_{10h} \quad (5)$$

Here, the factor a_1 takes into account the reliability and the factor a_{iso} the lubricant cleanliness. Both factors can be determined on the basis of the operating conditions and bearing parameters using the tables in the standard [ISO 281].

If the internal load distribution in the bearing is taken into account, the ISO/TS 16281 with the basic reference rating lifetime L_{10rh} can be used. In addition, ISO/TS 16281 considers the influences of bearing tilting and bearing clearance and can thus provide more precise information on life time. Similar to the modified rating lifetime L_{nmh}, the influences of cleanliness and reliability are also taken into account in the modified reference rating lifetime L_{nmrh} calculation by influencing factors. The calculated lifetimes for the operating conditions of the bearings investigated are given in Figure 12.

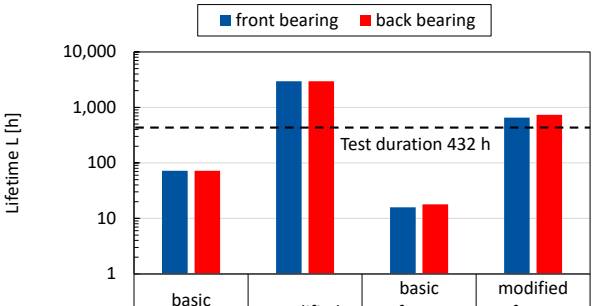

	basic rating lifetime L_{10h}	modified lifetime L_{nmh}	basic reference rating lifetime L_{10rh}	modified reference rating lifetime L_{nmrh}
front bearing	72	2,961	16	653
back bearing	72	2,961	18	734

Figure 12 : Calculated lifetime of the test bearings

According to the calculations, the basic rating lifetime is 72 h, the basic reference rating lifetime results in 16 h of operation. The modified lifetime L_{nmh} and the modified reference lifetime L_{nmh} are above the test duration of 432 h. This can be attributed to a positive influence due to the consideration of lubrication since the lubricant film thickness increases with increasing speed and thus wear is minimized. In addition the influence of surface fatigue, which is investigated in the tests, is not taken into account in the calculation methods of ISO 281 and ISO/TS 16281. The calculated values with the simulation software MTPlus do not provide a definitive statement on the actual lifetime, but they do illustrate that the operating conditions of the bearings in the test are significantly above the usual load limits.

4 CONCLUSIONS

The tests carried out show that the performance of the investigated new bearing steel for spindle bearings is significantly higher in comparison to spindle bearings with the standard steel 100Cr6. During the test runs the bearings showed a stable operating behaviour under a constant high load of 3 kN, a maximum contact pressure of 2,876 MPa of the inner ring, a rotational speed of 46 krpm and a speed parameter of 2.48 million mm/min. It can be assumed that the bearings with PM1 steel can be operated significantly longer under these conditions in comparison to the standard bearings. Differences in the steady state temperatures of the different tests can be attributed to differences in the bearing geometries on the bearing inner ring. The generally higher temperature level of the back bearings in the tests can be explained by the poorer heat dissipation of the larger housing parts of the back bearing. The vibration velocities of the prototype bearings are within the specified standard range, the vibration level with the reference bearings are above these specifications. An analysis of the operating conditions with regard to the contact pressures and the basic rating lifetime and basic reference rating lifetime show that the bearings were run in a critical operating condition and premature failure would have been expected under the test conditions. The microscope analyses and measured surface profile of the inner rings of the tested bearings showed no wear, which indicates a good resistance against surface fatigue and micropitting of the steels. Based on the stable operating behavior of all investigated bearings in endurance run, it can be stated that the load limits of hybrid spindle bearings with the new bearing steel (PM1) are significantly higher than originally assumed.

ACKNOWLEDGMENTS

The authors would like to thank SKF for permission to publish this paper.

REFERENCES

[Bayer 1998] Bayer, O. and Silverio, T. Increased Performance of High Speed Spindle Bearings. FAG Aircraft/Super Precision Bearings GmbH, 1998.

[Brecher 2019] Brecher, C.; Fey, M.; Falker, J.: Simulation schnell drehender Welle-Lager-Systeme - Teil 1. Antriebstechnik, 2019, Vol. 58, pp. 66–72.

[Brecher 2020] Brecher, C.; Neus, S.; Christoffers, D.: Dynamische Schmierzustandserkennung Oel-Luft-geschmierter Spindellager, ZWF - Werkzeugmaschinen, 2020, Vol. 115.

[Brecher 2017] Brecher, C.; Weck, M.: Werkzeugmaschinen Fertigungssysteme 2: Konstruktion, Berechnung und messtechnische Beurteilung, Springer, 2017, ISBN 978-3-662-46567-7.

[Catelbajac 2014] Catelbajac, C. de; Ritou, M.; Laporte, S.; Furet, B.: Monitoring of distributed defects on HSM spindle bearings. Applied Acoustics, 2014, Vol. 77, pp. 159–168.

[Falker 2020] Falker, J.: Analyse des Betriebsverhaltens von Hochgeschwindigkeits-Wälzlagern unter radialen Lasten. ISBN: 978-3-86359-799-3, Thesis, RWTH Aachen, 2020.

[Gerlach 2014] Gerlach, G.: Verbesserung des tribologischen Systems Spindellager im Hinblick auf kritische Schmierungszustände. RWTH Aachen, 2014.

[Heinz-Schwarzmaier 2003] Heinz-Schwarzmaier, T.: Bestimmung der Lebensdauer feststoffgeschmierter Kugellager auf der Grundlage von Reibenergieberechnungen und Kurzzeitvesuchen, Thesis, TU Darmstadt, 2003.

[Hentschke 2012] Hentschke, C.: Prognose des Verschleißverhaltens langsam laufender Wälzlager unter Berücksichtigung der Reaktionsschichtbildung, ISBN: 978-3-86130-599-6, Thesis, RWTH Aachen, 2012.

[ISO 10816-3] ISO 10816-3: Mechanical vibration — Evaluation of machine vibration by measurements on non-rotating parts — Part 3: Industrial machines with nominal power above 15 kW and nominal speeds between 120 r/min and 15 000 r/min when measured in situ, 2nd ed., 2009.

[Morales-Espejel 2021] Morales-Espejel, G. and Brizmer, V.: Effect of Materials and Surfaces on Frictional Heating Resistance of High-Speed High-Load Rolling Bearings. Part J: Journal of Engineering Tribology, 2021.

[Morales-Espejel 2019] Morales-Espejel, G.E.; Gabelli, A.: Rolling bearing seizure and sliding effects on fatigue life. Proceedings of the Institution of Mechanical Engineers, Part J: Journal of Engineering Tribology, 2019, Vol. 233, No. 2, pp. 339–354. ISSN 1350-6501.

[ISO 492:2014] ISO 492:2014: Rolling bearings — Radial bearings, Geometrical product specifications (GPS) and tolerance values, Beuth Verlag, 2014.

[Ragan 2002] Ragan, M. A.; Anthony, D. A.; Ronald, F. S.: A comparison of the mechanical and physical properties of contemporary and new alloys for aerospace bearing application, Bearing steel technology, ASTM STP 1419, J.M. Baeswick, Ed.; American Society for Testing and Materials International, West Conshohocken, PA, 2002.

[Rossaint 2013] Rossaint, J.: Steigerung der Leistungsfaehigkeit von Spindellagern durch optimierte Lagergeometrien, ISBN 978-3-86359-169-4, Thesis, RWTH Aachen, 2013.

[Sherif 2021] Sherif, M. Y.; Brizmer, V.; Meeuwenoord, R.; Matta, C.; Broitman, E.; Nuijten, T.: The Influence of Steel Microstructure in High-Speed High-Load Bearing Applications. Materials Science and Technology, 2021.

[SKF 2014] SKF: Super-precision bearings, https://www.skf.com/binaries/pub12/Images/0901d19680495562-Super-precision-bearings-catalogue---13383_2-EN_tcm_12-129877.pdf, 2014.

[Spachtholz 2008] Spachtholz, G.: Erweiterung des Leistungsbereiches von Spindellagern, ISBN-10: 9783940565136, Thesis, RWTH Aachen, 2008.

[ISO 281] International standard ISO 281, Rolling bearings – dynamic load ratings and rating life, 2nd ed.; 2007.

[ISO 16281] International standard ISO/TS 16281: Rolling bearings — Methods for calculating the modified reference rating life for universally loaded bearings, 1st ed.; 2008.

CONTACTS:

Marcus Gaertner, M. Sc.

Laboratory for Machine Tools and Production Engineering (WZL) of RWTH Aachen University

Campus-Boulevard 30, 52074 Aachen, Germany

+49 241 80 24791, m.gaertner@wzl.rwth-aachen.de, https://www.wzl.rwth-aachen.de